  Bull. Chem. Soc. Jpn., 59, 2717—2722 (1986)

Electrocatalytic Oxygen Reduction at (Tetrasulfonatophthalocyaninato)-cobalt Incorporated Polypyrrole Film Electrode

Tetsuya OSAKA,* Katsuhiko NAOI, Takayuki HIRABAYASHI, and Sadako NAKAMURA†
Department of Applied Chemistry, School of Science and Engineering, Waseda University, Shinjuku-ku, Tokyo 160
†Department of Chemistry, Japan Women's University, Mejirodai, Bunkyo-ku, Tokyo 112
(Received April 8, 1986)

Electrocatalytic activity of oxygen reduction was strikingly improved at a GC(glassy carbon)/PPy(polypyrrole)/CoTSP((tetrasulfonatophthalocyaninato)cobalt) electrode among the other CoTSP doped polymer electrodes. The GC/PPy/CoTSP electrode was formed by electro-oxidized polymerization of pyrrole on a glassy carbon(GC) electrode in methanol solution containing CoTSP. The catalytic oxygen reduction at the GC/PPy/CoTSP electrode was mainly analyzed with RRDE technique. Oxygen reduction reaction at the GC/PPy/CoTSP electrode in 0.05 mol dm^{-3} H_2SO_4 showed ca. 0.5 V more anodic onset potential than the value obtained with a GC electrode in 0.05 mol dm^{-3} H_2SO_4 containing 10^{-3} mol dm^{-3} CoTSP. Kouteckty-Levich plot, i.e., the relation between I_{lim}^{-1} and $\omega^{-1/2}$ for the GC/PPy/CoTSP electrode gave almost the same slope of theoretical four-electron reduction at the limiting current region. It was indicated that the apparent oxygen reduction is occurred through direct four-electron exchange process. On the other hand, the GC electrode in dissolved CoTSP gave almost the same slope as of theoretical two-electron reduction. A diagnostic criterion for oxygen reduction proposed by Wroblowa et al.[19] indicated that the parallel pathways of two- and four-electron reduction exist for the GC/PPy/CoTSP electrode.

Catalytic properties of macrocyclic transition metal complexes such as metal porphyrins and phtalocyanines for an electrochemical oxygen reduction have been recognized and examined extensively by many workers.[1,2] An active, inexpensive and also stable catalyst system, however, has not yet been discovered.[14-17] In this connection, special efforts have been made to enhance the activity of electrode catalysts such as graphite by modifying their surfaces with some active materials. Utilization of modified catalytic electrode at monolayer level has not been so successful in that they lack stability and conductivity in a doped state due to an unstable and insulating nature of adsorbed species on the substrate.[3-5] Recently, incorporation of electrocatalytic materials into polymer-coated electrode has been introduced as an easy and potential means for fixing a large metal complexes as active catalyst on a substrate.[6-9] Polymer films can be deposited on an electrode by electro-oxidized polymerization simultaneously with the incorporation of active materials from the supporting electrolyte.

In this paper, we mainly adopted polypyrrole for coating glassy carbon(GC) electrode by considering the following advantages. First, pyrrole can easily be polymerized and form a fairly stable film which adheres well to the substrate. Second, polypyrrole shows a good electronic conductivity, and can be an excellent current collector and an electron shuttle. Third, polymerized polypyrrole shows an easy incorporation of dopants during the film formation.

Bull et al.[6] reported that there was no remarkable change in catalytic activity by doping FeTSP in PPy film. However, a considerable improvement on catalytic activity of O_2 reduction was observed by doping [5,10,15,20-tetrakis(4-sulfonatophenyl)porphyrinato] metals such as CoTPPS, FeTPPS and MnTPPS in polypyrrole films.[7,8] In the previous communication,[9] we briefly surveyed some PPy modified metal porphyrins such as FeTPPS, CoTPPS, FeTSP, and CoTSP for the activity of O_2 reduction. Among these, we found that the GC/PPy/CoTSP electrode showed the highest activity with respect to an onset potential of O_2 reduction reaction. The main motivation of the paper is to throw a light on the interpretation of oxygen reduction mechanism for the GC/PPy/CoTSP electrode with RRDE (rotating ring-disk electrode) technique.

Experimental

CoTSP was synthesized and purified after an usual way,[10] and was then identified by an absorption spectrum using the same method in Refs.[11,12] Electrocatalytic activities for oxygen reduction reaction were mainly examined by rotating Pt ring–GC disk electrode (RRDE) at various rotating speeds. The ring and disk electrodes were pretreated by polishing with alumina grain (0.3 μmϕ) suspended in water. The ring-disk electrode was calibrated with the iron(II)/iron(III) couple. The value of collection efficiency, N, determined in this manner was 0.40 which was well consistent with the value of 0.40 obtained from the geometry of electrodes. An Ag/AgCl was used as a reference electrode and all the potentials for electrochemical measurements were referred to it. Pt wire was used as a counter electrode. Polymer coated CoTSP electrodes were deposited on GC by potentiostatic electropolymerization in methanol or aqueous solution containing CoTSP. The film thickness of polymer films was controlled by passing 90 mC cm^{-2}. GC/PPy/CoTSP and GC/PMP(poly(N-methylpyrrole))/CoTSP were formed at 1.2 V vs. Ag/Ag$^+$ in methanol solution containing 0.1 mol dm^{-3} monomer and 10^{-3} mol dm^{-3} CoTSP. GC/PPr(polypyrene)/CoTSP was formed at 1.2 V vs. Ag/Ag$^+$ in methanol containing

0.01 mol dm^{-3} monomer and 10^{-3} mol dm^{-3} CoTSP. GC/PAn(polyaniline)/CoTSP was formed at 0.8 V vs. Ag/AgCl in an aqueous solution containing 0.1 mol dm^{-3} monomer, 0.2 mol dm^{-3} H_2SO_4 and 10^{-3} mol dm^{-3} CoTSP. Solutions with various pH values were used as follows; 0.05 mol dm^{-3} H_2SO_4 (pH=1.2), 0.05 mol dm^{-3} $KH_2PO_4+5.6\times10^{-3}$ mol dm^{-3} NaOH (pH=6.0), and 0.025 mol dm^{-3} $Na_2HPO_4+3.3\times10^{-3}$ NaOH (pH=10.9). The intermediate hydrogen peroxide generated by two-electron reduction of O_2 was detected by ring electrode which was polarized at 1.10 V (pH=1.2), 0.82 V (pH=6.0), and 0.53 V (pH=10.9) while scanning the disk electrode potential at a scan rate of 10 mV s^{-1}.

Results and Discussion

Figure 1 shows typical O_2 reduction curves for GC/Polymer/CoTSP electrodes at 960 rpm where the background currents in N_2 atmosphere are already subtracted. GC/PPy/CoTSP, GC/PMP/CoTSP and GC/PAn/CoTSP electrodes have almost the same onset potentials at ca. 0.50 V which are the most favorable potential compared with the other two electrode systems, viz., GC/PPr/CoTSP and GC electrode in dissolved CoTSP. However, the ring current behavior of each electrode indicates that GC/PPy/CoTSP electrode is the most active oxygen reduction catalyst because of the occurrence of the four-electron transfer process to H_2O at the potential cathodic to 0.00 V. Therefore, the GC/PPy/CoTSP electrode was considered to be the most active oxygen reduction catalyst among the other polymer coated electrodes and worthwhile examining further.

Typical pH dependence of RRDE polarization curves for the GC/PPy/CoTSP is shown in Fig. 2. Oxygen reduction current at the GC/PPy/CoTSP disk electrode has onset potentials of ca. 0.50 V (pH=1.2), ca. 0.25 V (pH=6.0), and ca. 0.00 V

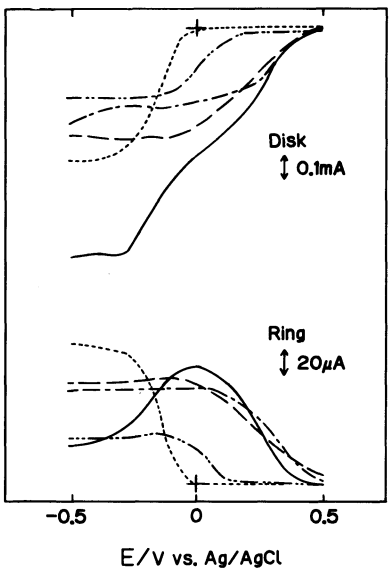

Fig. 1. Ring-disk current vs. potential curves for GC/CoTSP electrodes coated with various conductive polymers at 960 rpm in 0.05 mol dm^{-3} H_2SO_4. Film preparation conditions are indicated in the experimental section.
——: CoTSP/Polypyrrole, — — —: CoTSP/Poly(*N*-methylpyrrole) ——: CoTSP/Polyaniline, ——: CoTSP/Polypyrene, ------: GC electrode in 10^{-3} mol dm^{-3} CoTSP.

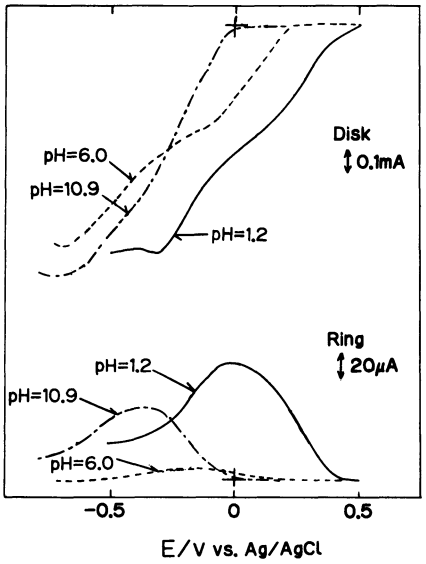

Fig. 2. pH dependence of RRDE curves for O_2 reduction at GC/PPy/CoTSP electrode at 960 rpm. pH=1.2 : 0.05 mol dm^{-3} H_2SO_4, pH=6.0 : 0.05 mol dm^{-3} $KH_2PO_4+5.6\times10^{-3}$ mol dm^{-3} NaOH, pH=10.9 : 0.025 mol dm^{-3} $Na_2HPO_4+3.3\times10^{-3}$ mol dm^{-3} NaOH.

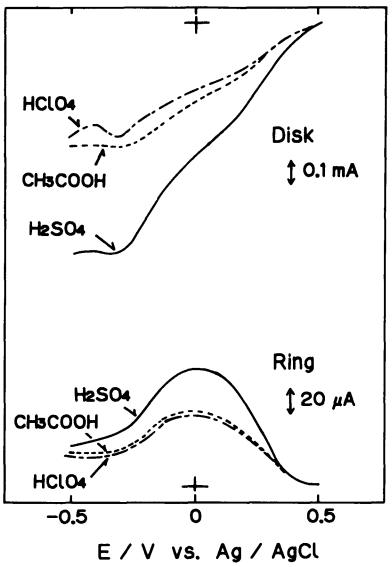

Fig. 3. Supporting electrolyte dependence of RRDE curves at GC/PPy/CoTSP electrode at 960 rpm. The pH values for all solutions were adjusted to 1.2.

(pH=10.9). As proton concentration increases, the onset potentials of O_2 reduction are observed to shift to the anodic side. In the solution of pH=1.2, the disk current shows the most anodic onset potential and a relatively clear limiting current is observed. The ring current shows a peak at ca. 0.00 V, and decreases until −0.32 V at which disk current exactly shows a maximum, and finally becomes constant current. At the potential more cathodic than 0.00 V, the four-electron process seems to occur. In the solution of pH=6.0, both disk and ring current curves have an onset potential at 0.25 V. Although disk current shows a substantial increase, the ring current shows almost zero change, indicating that the direct reduction from O_2 to H_2O is dominantly involved. In the solution of pH=10.9, the two- and the four-electron process seems to occur in parallel. The following study is focused on the behavior of GC/PPy/CoTSP electrode in the acidic solution of pH=1.2.

Figure 3 shows polarization curves for O_2 reduction reaction in three different supporting electrolytes, viz., H_2SO_4, CH_3COOH, and $HClO_4$ at pH=1.2. O_2 reduction current for H_2SO_4 electrolyte keeps the highest values than those in the other electrolyte. Polarization curves for O_2 reduction curves are observed to be very sensitive to the electrolyte anions used for the O_2 reduction measurements. The reason for that is still unclear at the present stage, but the behavior of polarization curves may have a close relationship with the mobility of anions in electrolyte solutions and the polymer film resistances with anion doped states.

Polarization curve of O_2 reduction at a GC/PPy electrode without CoTSP dopants and at the GC/PPy/CoTSP electrode are compared as shown in Fig. 4. As is evident from the disk currents, an onset potential for the GC/PPy electrode is 0.0 V, which is less anodic than that for the GC/PPy/CoTSP. Ring currents for the GC/PPy/CoTSP and the GC/PPy electrodes have onset potentials at 0.50 V and 0.00 V, respectively. For the GC/PPy/CoTSP electrode, two-electron reduction of O_2 is observed to occur at ca. 0.50 V, and has peak value at 0.00 V. At the potentials cathodic to 0.00 V, four-electron reduction gradually became to be involved. On the other hand, for the GC/PPy electrode, only two-electron O_2 reduction process occurs at the potential cathodic to 0.00 V. By incorporating CoTSP into PPy film, catalytic activity of O_2 reduction is found to be highly improved.

Oxygen Reduction Mechanism at GC/PPy/CoTSP Electrode. Figure 5 shows polarization curves for the GC/PPy/CoTSP electrode. Background currents for the GC/PPy/CoTSP electrode in N_2 atmosphere are almost the same for given range of rotation speeds. The background currents at given rotation speeds are already subtracted so that the polarization curves reflect only O_2 reduction reaction. At potentials from −0.2 V to −0.3 V, the polarization curves have the plateaus and can reasonably be understood as the limiting currents. Therefore, the Kouteckty-Levich plots can be applied to these curves. According to the

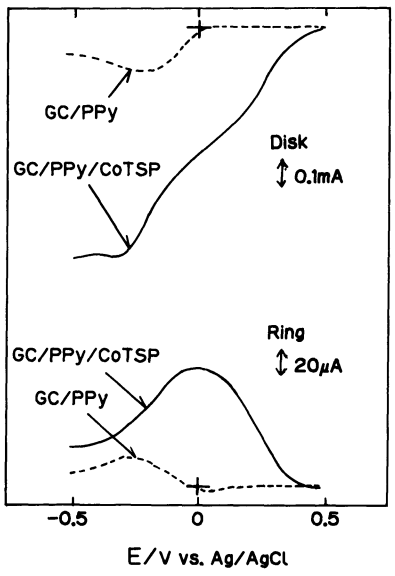

Fig. 4. Ring-disk current vs. potential curves for GC/PPy/CoTSP electrode (solid line) and GC/PPy (dashed line) formed at 1.2V vs. Ag/AgCl in 0.1 mol dm^{-3} Na_2SO_4+0.1 mol dm^{-3} pyrrole monomer at 960 rpm in 0.05 mol dm^{-3} H_2SO_4.

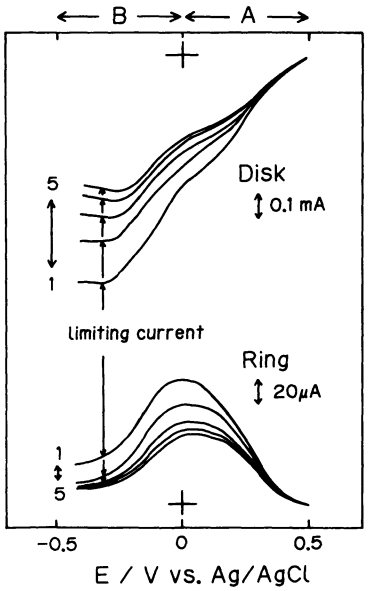

Fig. 5. Ring-disk current vs. potential curves for GC/PPy/CoTSP electrode at various rotation speeds in 0.05 mol dm^{-3} H_2SO_4 in O_2(solid lines) and N_2 (dashed line) atmosphere. The numbers 1, 2, 3, 4, and 5 correspond to 960, 610, 420, 310, and 240 rpm, respectively.

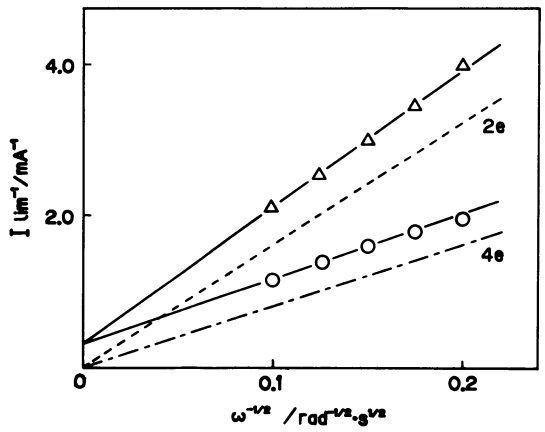

Fig. 6. Kouteckty-Levich plots for O_2 reduction reaction at GC/PPy/CoTSP electrode (—○—) and GC electrode in 10^{-3} mol dm^{-3} CoTSP (—△—) in 0.05 mol dm^{-3} H_2SO_4. Theoretical lines for two- and four-electron exchange reactions of O_2 reduction at bare electrode are indicated in the figure.

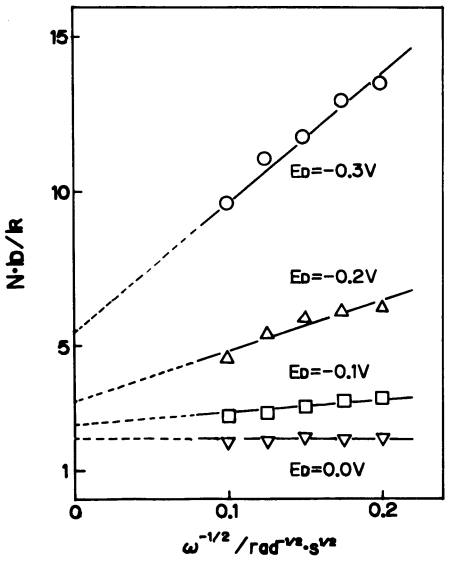

Fig. 7. NI_D/I_R vs. $\omega^{-1/2}$ plots for O_2 reduction reaction at GC/PPy/CoTSP electrode at various disk potentials in 0.05 mol dm^{-3} H_2SO_4. The disk potentials are indicated in the figure.

shape of ring currents, O_2 reduction mechanism can be discussed in two potential regions, viz., **A**: 0 V to 0.5 V, **B**: −0.50 V to 0 V. For the GC/PPy/CoTSP electrode in region **A**, O_2 reduction appears to occur from ca. 0.5 V, partly via H_2O_2, and the ring current steadily increases. In region **B**, the ring current of the GC/PPy/CoTSP electrode shows reverse behavior to that in region **A**, and the intermediate H_2O_2 gradually decreases for the GC/PPy/CoTSP electrode. It is assumed that O_2 reduction at the GC/PPy/CoTSP electrode partly became to involve four-electron transfer process at the transition potential region from **A** to **B**. Thus, for the GC/PPy/CoTSP electrode, the reaction path changed partly from two-electron process to four-electron process in this potential region.

Figure 6 shows the Kouteckty-Levich plots for the GC/PPy/CoTSP electrode and the GC electrode in dissolved CoTSP at the potential at which the limiting current was observed. The disk limiting current(I_{lim}) can generally be expressed as follows;[18]

$$1/I_{lim} = 1/I_k + 1/(I_d)_{lim} \quad (1)$$

$$(I_d)_{lim} = 0.62\,nFAD^{2/3}\nu^{-1/6}\omega^{1/2}Cb, \quad (2)$$

where $(I_d)_{lim}$, I_k, Cb, D, ν are the diffusion limiting current, the reaction controlled current, the dissolved O_2 concentration, the diffusion coefficient of O_2, the kinematic viscosity of the solution, respectively. Theoretical values for two- and four-electron reduction are calculated by using Eq.2 and the values of D and ν in Ref.[13] For both electrodes, the linear relationship between the reciprocal of limiting current and (rotation speed)$^{-1/2}$ are shown. The plot for the GC electrode in dissolved CoTSP is in good agreement with the theoretical two-electron reduction.

In contrast, for the GC/PPy/CoTSP electrode, the slope is almost the same as the theoretical four-electron reduction. The reaction controlled current is observed at the intercept with I_{lim} axis for the GC/PPy/CoTSP eletrode.

Figure 7 shows NI_D/I_R vs. $\omega^{-1/2}$ plots as a function of disk potentials. All plots yield straight lines with their intercepts above unity. The increase of the slope is observed with an increase of cathodic potential. Further information on an apparent electroreduction can be obtained from the diagnostic criterion suggested by Wroblowa et al.[19] By postulating a generalized scheme[19] for possible oxygen electroreduction at the GC/PPy/CoTSP, disk current(I_D) to ring current(I_R) ratio was derived as follows:

$$N(I_D/I_R) = 1 + 2k_1/k_2 + A + (k_{-5}/Zw^{1/2})A$$

where

$$A = (2k_1/k_2k_5)(k_{-2}+k_3+k_4) + (2k_3+k_4)/k_5 \quad (3)$$

$$Z = 0.62D^{2/3}\nu^{-1/6}$$

with N, D, ν, and ω are the collection efficiency, the diffusion coefficient of peroxide, the kinematic viscosity and the angular velocity of electrode. Equation 3 involves the two main reaction pathways, i.e., four-electron reduction to H_2O (k_1) and two-electron reduction to H_2O_2 (k_2). Adsorbed H_2O_2 proceeds to the following reactions; **1.** further two-electron reduction to H_2O(k_3), **2.** reoxidation to O_2(k_{-2}), **3.** catalytic decomposition of adsorbed H_2O_2 to O_2 and H_2O(k_4), **4.** desorption of adsorbed H_2O_2(k_5).

Equation 3 reduces to Eq. 4 with the intercept(J) and slope (s) of the NI_D/I_R vs. $\omega^{-1/2}$ plots.

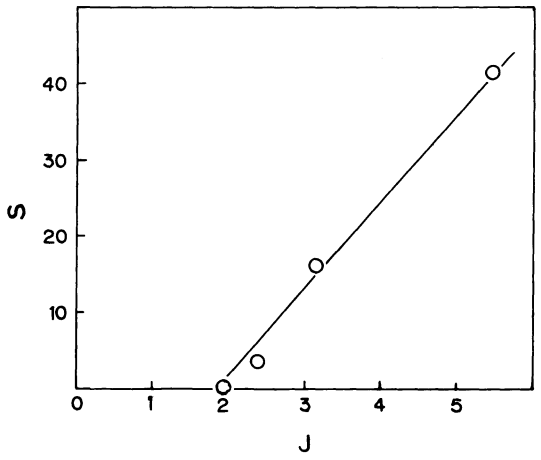

Fig. 8. Intercept(J) vs. slope (S) plot for O_2 reduction at GC/PPy/CoTSP electrode as a function of disk potentials.

$$J = 1 + 2k_1/k_2 + SZ/k_{-5} \quad (4)$$

Slope (S) was plotted against J at several disk potentials and indicated in Fig. 8. A straight line with the intercept $J'=2$ was yielded. When $k_1 \neq 0$, and k_1/k_2 is independent of potential, J vs. S plots should become linear with the intercept $J'>1$ as follows:

$$J' = 1 + 2k_1/k_2 \quad (5)$$

Hence, there is a parallel mechanism of four-electron direct reduction to H_2O and two-electron reduction to H_2O_2 process. The increase of S with an increase of cathodic potential is considered to be caused mainly by the occurrence of further oxidation from H_2O_2 to H_2O.

Cyclic Voltammograms for GC/PPy/CoTSP Electrode and GC Electrode in Dissolved CoTSP. One of the reasons of the high catalytic improvement for GC/PPy/CoTSP electrode would be deduced from the results in Fig. 9. In Fig. 9 a), a small redox peak was observed at around 0.3 V which may due to the redox reaction of CoTSP doped PPy film. The peaks are not so distinct because of the hindrance of PPy background, but they can be identified as ca. 0.31 V and ca. 0.22 V for anodic and cathodic peak potentials in N_2 atmosphere. The cathodic current peak at 0.22 V was increased when the solution was saturated with O_2. This catalytic reduction can be caused by the mediation effect of the redox couple at 0.30 V. As shown in Fig. 9b), O_2 reduction occurred at ca. 0.00 V which was far cathodic to the onset potential for the GC/PPy/CoTSP electrode. Therefore, the GC/PPy/CoTSP electrode has a favorable conditions with respect to the onset potential of O_2 reduction reaction. For the GC/PPy/CoTSP electrode, PPy matrix makes the redox potential more cathodic, which, as a result,

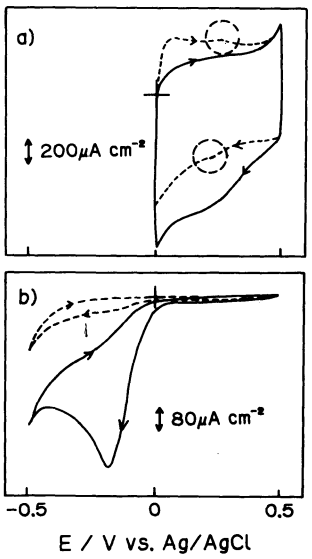

Fig. 9. Cyclic voltammograms for a) GC/PPy/CoTSP electrode and b) GC electrode in 10^{-3} mol dm^{-3} CoTSP at a scan rate of 50 mV s^{-1} in 0.05 mol dm^{-3} H_2SO_4 solution in O_2 (solid line) and N_2 (dashed line) atmosphere.

happen to form a favorable energy level of the CoTSP metal center for the formation of O_2 adduct with Co metal center of CoTSP.

The authors are indebted to Prof. Noboru Oyama and Dr. Takeo Ohsaka at Tokyo University of Agriculture and Technology for their valuable discussions and Mrs. Michiko Maeda at Japan Women's University for supplying CoTSP.

References

1) e.g., Proc. of Symp. on Electrocatalysis, ed by M. W. Breiter, Electrochem. Soc., 1974.

2) H. Behret, W. Clauberg, and G. Sandstede, *Z.Phys. Chem. NF*, **113**, 97 (1978).

3) A. Bettelheim, R. Parash, and D. Ozet, *J. Electrochem. Soc.*, **129**, 2247 (1982).

4) J. P. Collman, P. Denisevich, Y. Konai, M. Marroco, C. Koval, and F. C. Anson, *J. Am. Chem. Soc.*, **102**, 6027 (1980).

5) D. A. Butty and F. C. Anson, *J. Am. Chem. Soc.*, **106**, 59 (1984).

6) R. A. Bull, F. R. Fan, and A. T. Bard, *J. Electrochem. Soc.*, **131**, 687 (1983).

7) K. Okabayashi, O. Ikeda, and H. Tamura, *J. Chem. Soc., Chem. Commun.*, **1983**, 684.

8) O. Ikeda, K. Okabayashi, N. Yoshida, and H. Tamura, *J. Electroanal. Chem.*, **191**, 157 (1985).

9) T. Osaka, M. Nishikawa, and S. Nakamura, *Denki Kagaku*, **52**, 370 (1984).

10) J. H. Weber and D. H. Busch, *Inorg. Chem.*, **4**, 489 (1965).

11) L. D. Rollman and R. T. Iwamoto, *J. Am. Chem. Soc.*, **90**, 1455 (1968).

12) H. Kobayashi, Y. Torii, and N. Fukuda, *Nippon Kagaku Zasshi*, **81**, 694 (1960).
13) J. Zagal, P. K. Sen, and E. Yeager, *J. Electrochem. Soc.*, **87**, 207 (1977).
14) J. Zagal, P. Bindra, and E. Yeager, *J. Electrochem. Soc.*, **127**, 1506 (1980).
15) R. A. Bull, F. F. Fan, and A. J. Bard, *J. Electrochem. Soc.*, **129**, 1009 (1982).
16) A. Diaz, J. M. V. Vallejo, and A. M. Duran, *IBM J. Res. Develop.*, **25**, 42 (1981).
17) H. Behret, H. Binder, G. Sandante, and G. G. Scherer, *J. Electroanal. Chem.*, **117**, 29 (1981).
18) e.g., A. J. Bard and L. R. Faulkner, "Electrochemical Method, Fundametal and Application," Wiley, New York (1980).
19) H. S. Wroblowa, Y. CH. Pan, and G. Razumney, *J. Electroanal. Chem.*, **69**, 195 (1976).